

Accepted Manuscript

Highly selective catalytic hydroconversion of benzyloxybenzene to bicyclic cycloalkanes over bifunctional nickel catalysts

Xiao Zhou, Xian-Yong Wei, Zhong-Qiu Liu, Jing-Hui Lv, Yue-Lun Wang, Zhan-Ku Li, Zhi-Min Zong



PII: S1566-7367(17)30176-0
DOI: doi: [10.1016/j.catcom.2017.04.042](https://doi.org/10.1016/j.catcom.2017.04.042)
Reference: CATCOM 5027

To appear in: *Catalysis Communications*

Received date: 10 December 2016
Revised date: 15 April 2017
Accepted date: 23 April 2017

Please cite this article as: Xiao Zhou, Xian-Yong Wei, Zhong-Qiu Liu, Jing-Hui Lv, Yue-Lun Wang, Zhan-Ku Li, Zhi-Min Zong, Highly selective catalytic hydroconversion of benzyloxybenzene to bicyclic cycloalkanes over bifunctional nickel catalysts. The address for the corresponding author was captured as affiliation for all authors. Please check if appropriate. *Catcom*(2017), doi: [10.1016/j.catcom.2017.04.042](https://doi.org/10.1016/j.catcom.2017.04.042)

This is a PDF file of an unedited manuscript that has been accepted for publication. As a service to our customers we are providing this early version of the manuscript. The manuscript will undergo copyediting, typesetting, and review of the resulting proof before it is published in its final form. Please note that during the production process errors may be discovered which could affect the content, and all legal disclaimers that apply to the journal pertain.

Highly selective catalytic hydroconversion of benzyloxybenzene to bicyclic cycloalkanes over bifunctional nickel catalysts

Xiao Zhou, Xian-Yong Wei*, Zhong-Qiu Liu, Jing-Hui Lv, Yue-Lun Wang, Zhan-Ku Li, Zhi-Min Zong

Key Laboratory of Coal Processing and Efficient Utilization, Ministry of Education, China

University of Mining & Technology, Xuzhou 221116, Jiangsu, China

* Corresponding author. Tel: +86 516 83885951; fax: +86 516 83884399.
E-mail address: wei_xianyong@163.com (X. Y. Wei)

ABSTRACT

An active bifunctional nickel catalyst was prepared by decomposing $\text{Ni}(\text{CO})_4$ to highly dispersed metallic Ni onto H β zeolite and first applied in hydroconversion of benzyloxybenzene (BOB), which was used as a lignin model compound. Ni/H β was found to be effective for converting BOB into bicyclic cycloalkanes via C_{alk}-O bond cleavage induced by H⁺ addition, benzylium addition to 2- and 4-positions in phenol, hydrogenation of benzene ring, dehydration, and H⁻ abstraction. Compared to one-step conversion, the conversion of BOB was pretreated under N₂ atmosphere and then proceeded under H₂ atmosphere and a much higher selectivity of bicyclic cycloalkanes is obtained.

Keywords: Nickel; Benzyloxybenzene; Bicyclic cycloalkanes; Hydroconversion

1. Introduction

Lignin, a main constituent of lignocellulosic biomass (15–30% by weight, 40% by energy), has been a promising raw material for obtaining high-grade hydrocarbon fuels in view of its inherent phenylpropane based structure [1,2]. The catalytic treatments of lignin or lignin oligomers [3-8], especially **catalytic hydroconversion (CHC)** [9-12], have been extensively studied with the aim of producing fuel range hydrocarbons.

Due to the structural complexity of lignin, insight into the reactions of model compounds has become a powerful approach for elucidating the mechanism of **CHC** [13-21]. The **CHC** of **benzyloxybenzene (BOB)** representing α -O-4 linkages in lignin has been extensively investigated [11,17-21]. Zhao et al. examined **CHC** of **BOB** over Ni/HZSM-5 at 250 °C under 5 MPa of H₂. They found that **BOB** was selectively converted to monocyclic **cycloalkanes (MCCs)** with a yield of more than 98% and **bicyclic cycloalkanes (BCCs)** accounting for less than 2% [11]. Chen et al. investigated **CHC** of **BOB** in pseudo-homogeneous systems, *i. e.*, uniformly stabilized noble metal nanoparticles in ionic liquids, at 130 °C under 5 MPa of H₂ for 10 h. They found that cyclohexane (**CH**) and methylcyclohexane (**MCH**) were the main products with a small amount of **BCCs** [17]. Güvenatam et al. reported their investigation on aqueous phase **CHC** of **BOB** using noble metal catalysts (Pt, Pd, and Ru) at 200 °C under acidic conditions. Their results showed that the reaction predominantly yielded **CH** and **MCH** and the selectivity of **BCCs** was low [20]. The above **CHC** processes are accompanied by catalytic cleavage of **C-O ether bonds**, which results in the conversion of **BOB** into **MCCs**. These **MCCs** usually have a moderate value in fuel utilization [12]. Even though high value **BCCs** could be generated via two-step **CHC** of **BOB** [22], it requires two

specific catalysts which will increase the cost. However, to our knowledge, no reports have been issued on the CHC of BOB to high value BCCs on a sole catalyst and the bifunctional nickel catalysts prepared from $\text{Ni}(\text{CO})_4$ is rarely applied in CHC of BOB.

In the present study, we report a highly active bifunctional nickel catalyst, prepared by decomposing $\text{Ni}(\text{CO})_4$ to highly dispersed metallic Ni onto H β zeolite, for converting BOB under mild conditions to BCCs in *n*-hexane with high selectivity for the first time. The reaction route to BCCs may be useful to selectively produce high value jet fuels.

2. Experimental

2.1. Catalyst preparation

$\text{Ni}(\text{CO})_4$ was synthesized by reacting Ni powder with CO under 6.0MPa at 100 °C in a 100 mL stainless steel and magnetically stirred autoclave. All the 10 wt% Ni-based catalysts were prepared by dispersing 2 g of the catalyst support (activated carbon (AC), HZSM-5, H β , and HY) into a mixture of 30 mL diethyl ether and 1 mL $\text{Ni}(\text{CO})_4$ in the autoclave. After replacing air inside the autoclave with N_2 for three times, the mixture was stirred for 1 h at room temperature, and then the autoclave was heated to 100 °C and kept at the temperature for 1 h to allow dispersing of metallic Ni onto the support.

2.2. Catalyst characterizations

X-ray diffractometer (XRD) measurement was carried out with a Bruker Advance D8 XRD equipped with a Cu K α source ($\lambda=1.5406\text{\AA}$). N_2 adsorption-desorption isotherms were recorded by nitrogen adsorption at 77 K with an Autosorb-1-MP apparatus and the pore size distribution was calculated by the DFT method. Transmission electron microscope (TEM) analysis was performed with a JEM-1011 microscope. NH_3 temperature-programmed desorption (TPD) was performed on a

TP-5000 type multi-function adsorption instrument. X-ray photoelectron spectra (XPS) were taken on a Thermo Fisher Scientific K-Alpha 1063 spectrophotometer with the Al K α radiation and the beam spot size of 900 μm (energy step size 1.000 eV, pass energy 50.0 eV). Accurate binding energies could be determined by referring to the C 1s peak at 284.8 eV.

2.3. Catalytic reaction

In a typical run, 0.1 g BOB, 0.05 g catalyst, and 10 mL *n*-hexane were fed into a 60 mL stainless steel and magnetically stirred autoclave. After replacing air in the autoclave and pressurizing with H₂ or N₂ to 4 MPa at room temperature, the autoclave was heated to 160 °C followed by maintained at 160 °C for a prescribed period of time. Alternatively, the conversion of BOB was pretreated under N₂ atmosphere at 160 °C for 10 min and then proceeded under H₂ atmosphere at 160 °C for 2 h in the same autoclave mentioned above. The reaction mixture was taken out of the autoclave and filtrated after cooling the autoclave to the room temperature. The filtrate was identified with an Agilent 7890/5975 gas chromatograph/mass spectrometer. The quantification was performed with an Agilent 7890 gas chromatograph using *n*-decane as the external standard.

3. Results and Discussion

3.1. *CHC* of BOB

It is well-known that the catalyst supports play an essential role in governing product distribution [23], and thereby it is crucial to select a suitable support when preparing an active *CHC* catalyst. The catalytic performances of Ni-based catalysts with different supports were compared in *CHC* of BOB under mild condition (160 °C, 4 MPa of H₂, and 2 h), and the results are listed in Table 1. The high conversion of BOB (95.5%) and the low selectivity of cycloalkanes (29.9%) are achieved over Ni/AC. For Ni/HZSM-5, both the conversion of BOB and the selectivity of cycloalkanes are low.

Ni/HY presents the low selectivity of cycloalkanes, which is similar to Ni/AC and Ni/HZSM-5. Comparatively, the high conversion of BOB (100%) and the high selectivity of cycloalkanes (93.0%) are achieved over Ni/H β , indicating the superior catalytic performance in CHC of BOB. It is noteworthy that BCCs appear in the products over Ni/H β and Ni/HY and the highest selectivity of BCCs (68.3%) is obtained over Ni/H β . The excellent selectivity of BCCs is disclosed for the first time in one-step CHC of BOB.

Taking catalytic performance into account, Ni_{10%}/H β was chosen to study the effect of different periods of reaction time. As Table 2 displays, the Ni/H β -catalyzed converting of BOB is very fast. The conversion is 80.1% after 10 min and the conversion is complete after 30 min. As reaction time is extended, the selectivity of CH and MCH rises slightly, while the selectivity of phenol and toluene declines slowly, indicating that the latter two act as intermediates and are converted into the former two during this CHC process. Meanwhile, the selectivity of dicyclohexylmethane (DCHM) and cyclopentylethylcyclohexane (CPEC) increases noticeably, while the selectivity of 2-benzylphenol (2-BPH) and 4-benzylphenol (4-BPH) decreases obviously, also indicating that the latter two are converted into the former two during this CHC process. Moreover, the selectivity of DCHM and CPEC as BCCs rises much faster than that of CH and MCH as MCCs and the highest selectivity of BCCs is obtained after 90 min.

3.2. Catalyst characterizations

As illustrated in Table S1 and Fig. S1, HY has the largest specific surface area (SSA) and a relatively low total pore volume (TPV), the SSA and TPV of AC and HZSM-5 are low, whereas H β presents a high SSA and the highest TPV. The three zeolites show the ordered pore structure and the pore size is mainly in the range of 0-2.0 nm and slightly in the range of 2.0-4.0 nm, demonstrating

the presence of a large portion of the micropores along with a little amount of mesopores, whereas the pore size distributions of AC is broad and it demonstrates relatively more micropores. H β and Ni_{10%}/H β exhibit the similar shape of N₂ adsorption–desorption isotherm and pore size distribution, indicating that the textural property of H β is largely preserved after impregnation. The SSA of H β falls down from 534 to 502 m² g⁻¹ and the TPV decreases from 0.45 to 0.41 cm³ g⁻¹ after supporting metallic Ni. These may be due to the blocking of the microchannels by part of Ni species or the 10% less H β present in Ni_{10%}/H β . The similar results are also obtained over other supported Ni-based catalysts.

As XRD patterns presented in Fig. 1, the characteristic diffraction peaks are observed for all the catalysts at $2\theta = 44.5^\circ$, 51.8° , and 76.4° , corresponding to the (111), (200), and (220) crystallographic planes of face centered cubic Ni phase, respectively [24]. The intensity in the diffraction pattern of Ni_{10%}/H β is very weak, indicating the high dispersion of Ni species on the H β surface. The diameter of Ni (111) is calculated from the Scherrer equation as 18.6 nm, based on the XRD patterns of Ni_{10%}/H β .

As TEM images shown in Fig. S2, Ni particles dispersed uniformly on the H β in the Ni_{10%}/H β image. Analysis of this Ni fraction showed that the average Ni particle size is 19 nm as determined by transmission electron microscopy, which is quite consistent with the analysis with XRD.

As Fig. 2 exhibits, C, Si, Al, Ni, and O exist in Ni_{10%}/H β . The principal peaks in the range of 846–866 eV are attributed to Ni 2p_{3/2}. Among them, the peak at 861.4 eV is the satellite peak of NiO and the peak at 852.4 eV is assigned to metallic Ni, while the other 2 peaks at 856.0 and 854.4 eV denote the chemical bonds of NiO interacting strongly with the support and NiO dispersed on the

support [25], respectively. The existence of NiO species could be due to the easy oxidation of metallic Ni, which inevitably contacts with the air during the sample preparation and settlement. Furthermore, XPS of Ni/HZSM-5, Ni/HY, and Ni/AC were also investigated. As Fig. S3 demonstrates, the existence of Ni species in Ni/HZSM-5, Ni/HY, and Ni/AC is similar with that in Ni/H β . In comparison with the binding energy (BE) of metallic Ni in pure Ni powder [26] and Ni/AC (853.1 eV), the BE of metallic Ni in Ni/H β negatively shifted by 0.7 eV. According to the law of chemical shift, partial electron might transfer from H β to metallic Ni, leading to Ni slightly electron-enriched, which agreed with earlier investigation [27]. Generally, the adsorption of C=C group on the Ni catalyst follows a $d-\pi$ feedback mechanism and such electronic modifications would be favorable for the electron-donation to π^* -orbital and weaken the strength of C=C bond [26], which could facilitate the hydrogenation of C=C group [26,28].

As Fig. 3 demonstrates, the main NH₃ desorption peak centered at 183 °C and only a small hump centered at 565 °C were observed in the spectrum of HZSM-5, assigned to the weak and strong acidic sites, respectively. For H β , the NH₃ desorption peak location is at 189 °C with a broad shoulder peak appearing between 300 °C and 400 °C, demonstrating that both the weak and medium acidic sites appear simultaneously on this zeolite. For HY, the NH₃ desorption peak corresponding to the weak acidic sites appears at 196 °C, while the medium and strong acidic sites are not obvious. With medium acidity introduced, the catalytic activity of CHC for Ni/H β is significantly enhanced and the promotion effect can be attributed to the synergistic effect between metallic Ni and H β zeolite [29]. The increased medium acidic sites over Ni/H β seem to be generated from acidic [Ni(OH)⁺] group [30].

3.3. Mechanism for CHC of BOB

In the absence of Ni, the reaction predominantly yields 2-BPH (82.0%), 4-BPH (8.9%), and phenol (5.2%) over H β at 160 °C and 4MPa H₂ for 2 h. The selectivity of other products such as trimeric compounds and toluene is low. It is proposed that the 2 major products, 2- and 4-BPH, are obtained by acid-catalyzed C_{alk}-O bond cleavage to produce phenol and benzylium and benzylium addition to 2- and 4-positions in phenol. The third product, phenol, is obtained via acid-catalyzed C_{alk}-O bond cleavage. It is impossible for benzylium to abstract H[•] over H β during this process and the missing benzylium may contribute to the formation of dibenzylphenols. The conversion of BOB was also performed under N₂ atmosphere over Ni_{10%}/H β and the results are shown in Table S2. 2-BPH, 4-BPH, and phenol are also the main products and the product distribution is similar with the H β -catalyzed reaction in all the observed instances, which could further confirm our assumption that BOB is rearranged to 2- and 4-BPH over the acid sites of Ni_{10%}/H β .

It was reported that benzyl radicals could attack the naphthalene ring in 1-benzyl-naphthalene hydrocracking [31]. The aromatic rings are rich in electrons and the hydroxyl group makes the benzene rings more electronic. Moreover, benzyliums are electron deficient and the tendency of benzyliums to attack aromatic rings is stronger than that of benzyl radicals. Active metals, such as Fe, Ni, and Pd, proved to be effective for catalyzing the formation of H[•]-H [32,33]. In the presence of an acidic catalyst, H₂ can be heterolytically split to an immobile H⁻ adhered to the catalyst surface and a mobile H⁺ [34]. Since H[•]-H bond is weaker than H-H bond in H₂, heterolytically splitting H[•]-H bond to produce the mobile H⁺ is easier. As a result, Ni/H β can activate H₂ to H[•]-H and facilitate the heterolytical splitting of H[•]-H to a mobile H⁺ and immobile H⁻, as shown in Scheme 1.

Based on the above analyses, the possible mechanism for CHC of BOB under H₂ atmosphere over Ni/H β is depicted in Scheme 1. The conversion of BOB over Ni/H β mainly proceeds via

$C_{alk}-O$ bond cleavage induced by H^+ addition to produce phenol and benzylium, benzylium addition to 2- and 4-positions in phenol to produce 2- and 4-benzylphenols, hydrogenation of the benzylphenols to (cyclohexylmethyl)cyclohexanols, dehydration of (cyclohexylmethyl)cyclohexanols to (cyclohexylmethyl)cyclohexyliums, and abstraction of H^- from $Ni/H\beta$ surface by (cyclohexylmethyl)cyclohexyliums to DCHM. The conversion of BOB over $Ni/H\beta$ minorly proceeds via $C_{alk}-O$ bond cleavage induced by H^+ addition to produce phenol and benzylium and abstraction of H^- from $Ni/H\beta$ surface by benzylium to toluene followed by CHC of the resulting phenol and toluene to produce CH and MCH. The resulting benzyliums from the $C_{alk}-O$ bond cleavage attack the 2,6- and 2,4-positions of phenol to produce 2,6-dibenzylphenol (2,6-DBP) and 2,4-dibenzylphenol (2,4-DBP), respectively, followed by the dibenzylphenols hydrogenation along with subsequent dehydration and H^- abstraction to yield 1,3-bis(cyclohexylmethyl)cyclohexane (1,3-BCMC).

3.4. Reusability of $Ni_{10\%}/H\beta$ for CHC of BOB

To investigate the reusability of catalyst, the separated $Ni_{10\%}/H\beta$ was washed by acetone and dried under vacuum at 50 °C for 4 h. Without other treatments, $Ni_{10\%}/H\beta$ was used repeatedly for CHC of BOB at 160 °C, 4 MPa of H_2 , and 2 h. As Fig. S4 depicts, both the BOB conversion and the selectivity of BCCs dropped from the initial 100% and 68.3% to 90.1% and 48.6%, respectively, after the catalyst was reused for 3 recycles. TEM image of the recycled catalyst illustrates that the main reason for the decrease of catalyst activity is the aggregation of Ni particles on the catalyst surface (Fig. S5). However, the carbon deposition on the surface of catalyst is also supposed to influence the activity of $Ni/H\beta$ relatively.

3.5. CHC of BOB with the pretreatment under N_2 atmosphere

Because of the high selectivity for intermediate of benzylphenols over Ni/H β under N₂ atmosphere, a novel approach to producing more BCCs, namely, indirect CHC (ICHC), was presented. IHC of BOB was carried out over Ni_{10%}/H β at 160 °C and 4MPa N₂ for 10 min. Then, the products from the first step were subjected to IHC process over Ni_{10%}/H β at 160 °C and 4MPa H₂ for 2 h, producing DCHM (71.1%), CPEC (11.1%), CH (5.2%), MCH (0.6%), and 1,3-BCMC (4.6%) (Process I in Table S3). However, a one-step reaction, namely, direct CHC (DCHC), was performed over Ni_{10%}/H β at 160 °C and 4MPa H₂ for 2 h, which produces DCHM (52.6%), CPEC (15.7%), CH (7.8%), MCH (3.5%), and 1,3-BCMC (4.7%) (Process II in Table S3). BCCs account for 82.2% and 68.3% in the products from IHC and DCHC process, respectively. The difference in selectivity of BCCs can be attributed to the suppression to the abstraction of H⁺ from Ni/H β surface by benzylium under N₂ atmosphere in IHC.

4. Conclusions

In conclusion, bifunctional Ni/H β exhibits a high activity for CHC of BOB due to the synergistic effect between metallic Ni and H β zeolite. The highest selectivity of BCCs accounting for 68.3% is obtained in one-step CHC for the first time. The possible mechanism is that H⁺ attacks BOB to produce phenol and benzylium and benzylium adds to 2- and 4-positions in phenol to produce benzylphenols followed by the benzylphenols hydrogenation along with subsequent dehydration and H⁺ abstraction to yield BCCs over Ni/H β . Moreover, the conversion of BOB proceeded under N₂ atmosphere then H₂ atmosphere, yielding a much higher selectivity of BCCs. These results indicate that CHC process with the pretreatment under N₂ atmosphere, which can effectively suppress the abstraction of H⁺ from Ni/H β surface, might be useful to selectively produce BCCs as high value jet fuels from lignin.

Acknowledgements

This work was subsidized by the Key Project of Joint Fund from National Natural Science Foundation of China and the Government of Xinjiang Uygur Autonomous Region (Grant U1503293) and the Program of University in Jiangsu Province for Graduate Student's Innovation in Science Research (Grant KYLX15_1414).

References

- [1] J. Zakzeski, P.C.A. Bruijninx, A.L. Jongerius, B.M. Weckhuysen, *Chem. Rev.* 110 (2010) 3552-3599.
- [2] D.M. Alonso, S.G. Wettstein, J.A. Dumesic, *Chem. Soc. Rev.* 41 (2012) 8075-8098.
- [3] V.M. Roberts, V. Stein, T. Reiner, A. Lemonidou, X. Li, J.A. Lercher, *Chem. Eur. J.* 17 (2011) 5939-5948.
- [4] R. Ma, W.Y. Hao, X.L. Ma, Y. Tian, Y.D. Li, *Angew. Chem. Int. Ed.* 53 (2014) 7310-7315.
- [5] A.K. Deepa, P.L. Dhepe, *ACS Catal.* 5 (2015) 365-379.
- [6] J.A. Onwudili, P.T. Williams, *Green Chem.* 16 (2014) 4740-4748.
- [7] A.L. Jongerius, P.C.A. Bruijninx, B.M. Weckhuysen, *Green Chem.* 15 (2013) 3049-3056.
- [8] J. Zhang, J. Teo, X. Chen, H. Asakura, T. Tanaka, K. Teramura, N. Yan, *ACS Catal.* 4 (2014) 1574-1583.
- [9] S.K. Singh, J.D. Ekhe, *RSC Adv.* 4 (2014) 27971-27978.
- [10] M. Saidi, F. Samimi, D. Karimipourfard, T. Nimmanwudipong, B.C. Gates, M.R. Rahimpour, *Energy Environ. Sci.* 7 (2014) 103-129.
- [11] C. Zhao, J.A. Lercher, *Angew. Chem. Int. Ed.* 51 (2012) 5935-5940.
- [12] H.L. Wang, R. Hao, H.S. Pei, H.M. Wang, X.W. Chen, M.P. Tucker, J.R. Cort, B. Yang, *Green*

Chem. 17 (2015) 5131-5135.

- [13] N. Yan, Y.A. Yuan, R. Dykeman, Y.A. Kou, P.J. Dyson, *Angew. Chem. Int. Ed.* 49 (2010) 5549-5553.
- [14] Y. Hong, H. Zhang, J. Sun, K.M. Ayman, A.J. Hensley, M. Gu, M.H. Engelhard, J.-S. McEwen, Y. Wang, *ACS Catal.* 4 (2014) 3335-3345.
- [15] A. Gutierrez, R.K. Kaila, M.L. Honkela, R. Slioor, A.O.I. Krause, *Catal. Today* 147 (2009) 239-246.
- [16] D.Y. Hong, S.J. Miller, P.K. Agrawal, C.W. Jones, *Chem. Commun.* 46 (2010) 1038-1040.
- [17] L. Chen, J. Xin, L. Ni, H. Dong, D. Yan, X. Lu, S. Zhang, *Green Chem.* 18 (2016) 2341-2352.
- [18] C. Zhao, J.A. Lercher, *ChemCatChem* 4 (2012) 64-68.
- [19] J.D. Adjaye, N.N. Bakhshi, *Biomass Bioenergy* 8 (1995) 131-149.
- [20] B. Güvenatam, O. Kurşun, E.H.J. Heeres, E.A. Pidkova, E.J.M. Hensen, *Catal. Today* 233 (2014) 83-91.
- [21] J.Y. He, L. Lu, C. Zhao, D.H. Mei, J.A. Lercher, *J. Catal.* 311 (2014) 41-51.
- [22] J.S. Yoon, Y. Lee, J. Ryu, Y.A. Kim, E.D. Park, J.W. Choi, J.M. Ha, D.J. Suh, H. Lee, *Appl. Catal. B Environ.* 142-143 (2013) 668-676.
- [23] Y.X. Wang, Y.M. Fang, T. He, H.Q. Hu, J.H. Wu, *Catal. Commun.* 12 (2011) 1201-1205.
- [24] G.S. Fu, Y. He, Y.W. Zhang, Y.Q. Zhu, Z.H. Wang, K.F. Cen, *Energy Convers. Manage.* 117 (2016) 520-527.
- [25] Z. Boukha, M. Kacimi, M.F.R. Pereira, J.L. Faria, J.L. Figueiredo, M. Ziyad, *Appl. Catal. A Gen.* 317 (2007) 299-309.
- [26] H. Li, H. Li, W. Dai, M. Qiao, *Appl. Catal. A Gen.* 238 (2003) 119-130.

- [27] D. Dutta, D.K. Dutta, Appl. Catal. A Gen. 487 (2014) 158-164.
- [28] H. Li, H. Li, J. Deng, Appl. Catal. A Gen. 193 (2000) 9-15.
- [29] H.L. Zuo, Q.Y. Liu, T.J. Wang, L.L. Ma, Q. Zhang, Q. Zhang, Energy Fuels 26 (2012) 3747-3755.
- [30] B.I. Mosqueda-Jiménez, A. Jentys, K. Seshan, J.A. Lercher, J. Catal. 218 (2003) 375-385.
- [31] X.Y. Wei, E. Ogata, E. Niki, Sekiyu Gakkaishi 35 (1992) 358-361.
- [32] X.Y. Wei, E. Ogata, Z.M. Zong, S.L. Zhou, Z.H. Qin, J.Z. Liu, K. Shen, H.Q. Li, Fuel Process. Technol. 62 (2000) 103-107.
- [33] X.Y. Wei, Z.H. Ni, Z.M. Zong, S.L. Zhou, Y.C. Xiong, X.H. Wang, Energy Fuels 17 (2003) 652-657.
- [34] X.M. Yue, X.Y. Wei, B. Sun, Y.H. Wang, Z.M. Zong, X. Fan, Z.W. Liu, Appl. Catal. A Gen. 425-426 (2012) 79-84.

Figure captions

Fig. 1. XRD patterns of H β zeolite and supported Ni catalysts.

Fig. 2. XPS and fitting curve of Ni 2 $p_{3/2}$ for Ni_{10%}/H β .

Fig. 3. NH₃-TPD profiles for different acidic zeolites and Ni_{10%}/H β .

Scheme 1. Possible pathways for CHC of BOB under H₂ atmosphere over Ni_{10%}/H β .

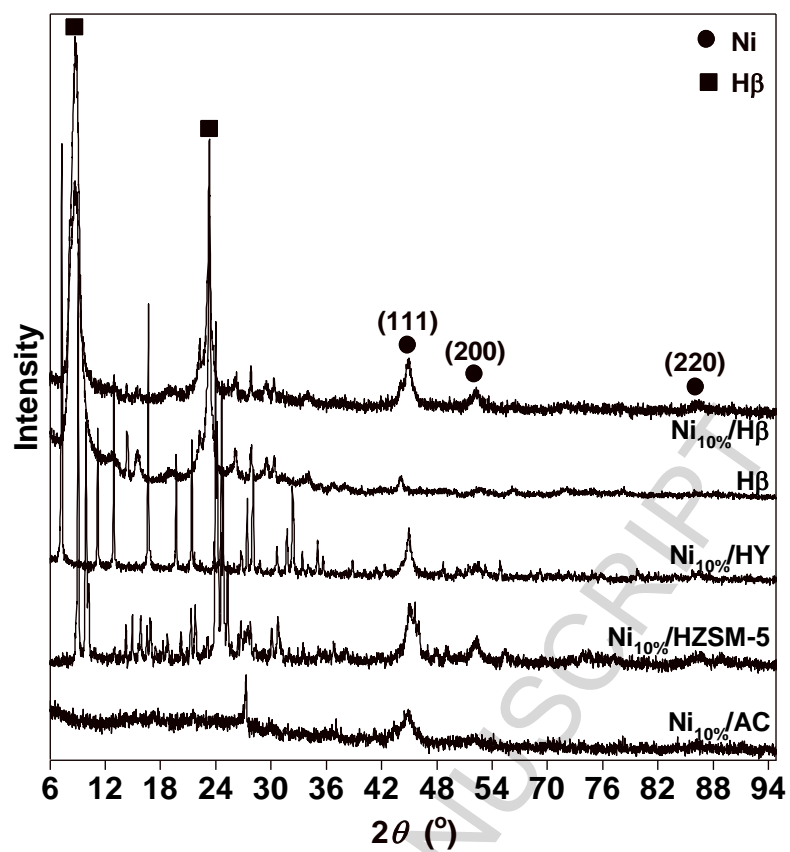


Fig. 1. XRD patterns of Hβ zeolite and supported Ni catalysts.

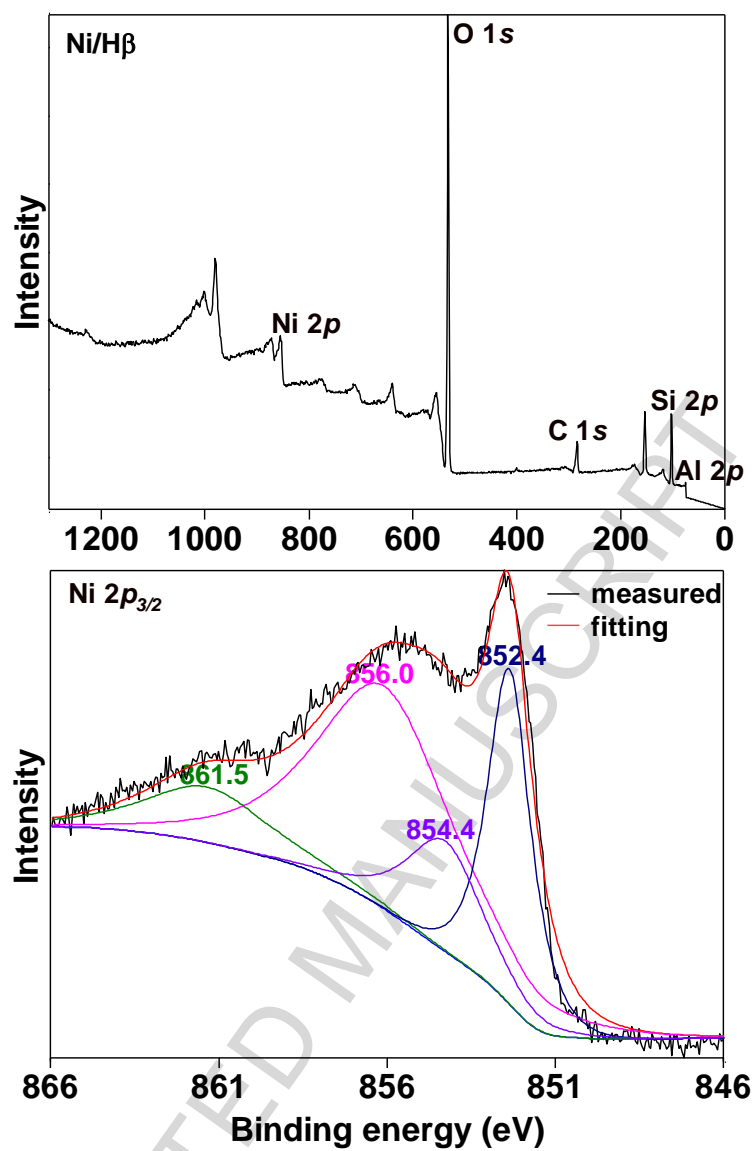


Fig. 2. XPS and fitting curve of Ni 2p_{3/2} for Ni_{10%}/Hβ.

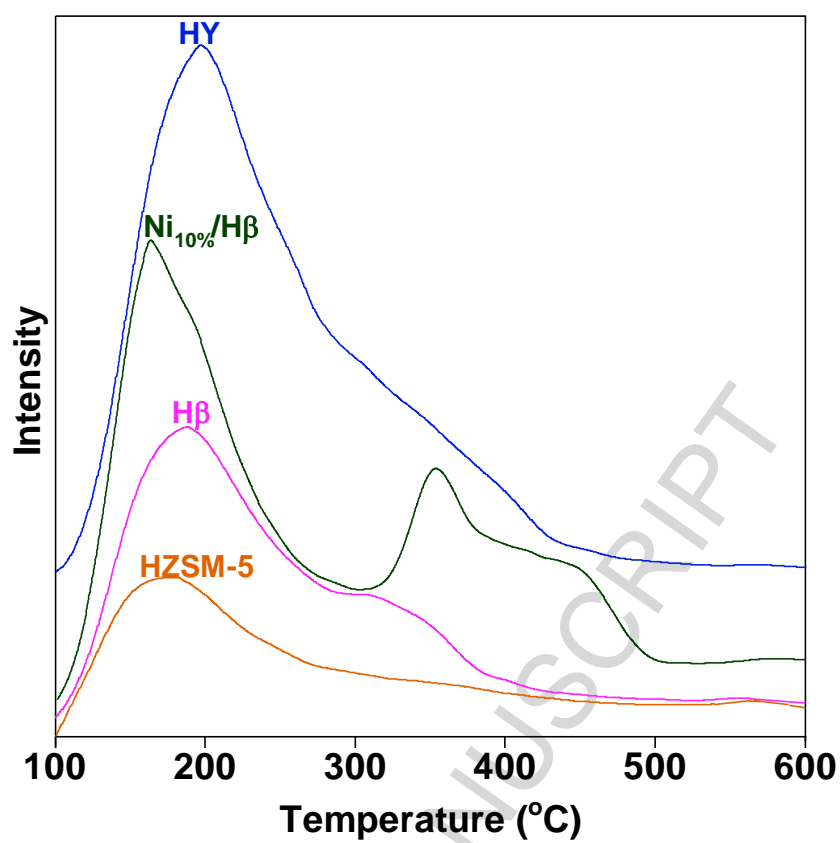
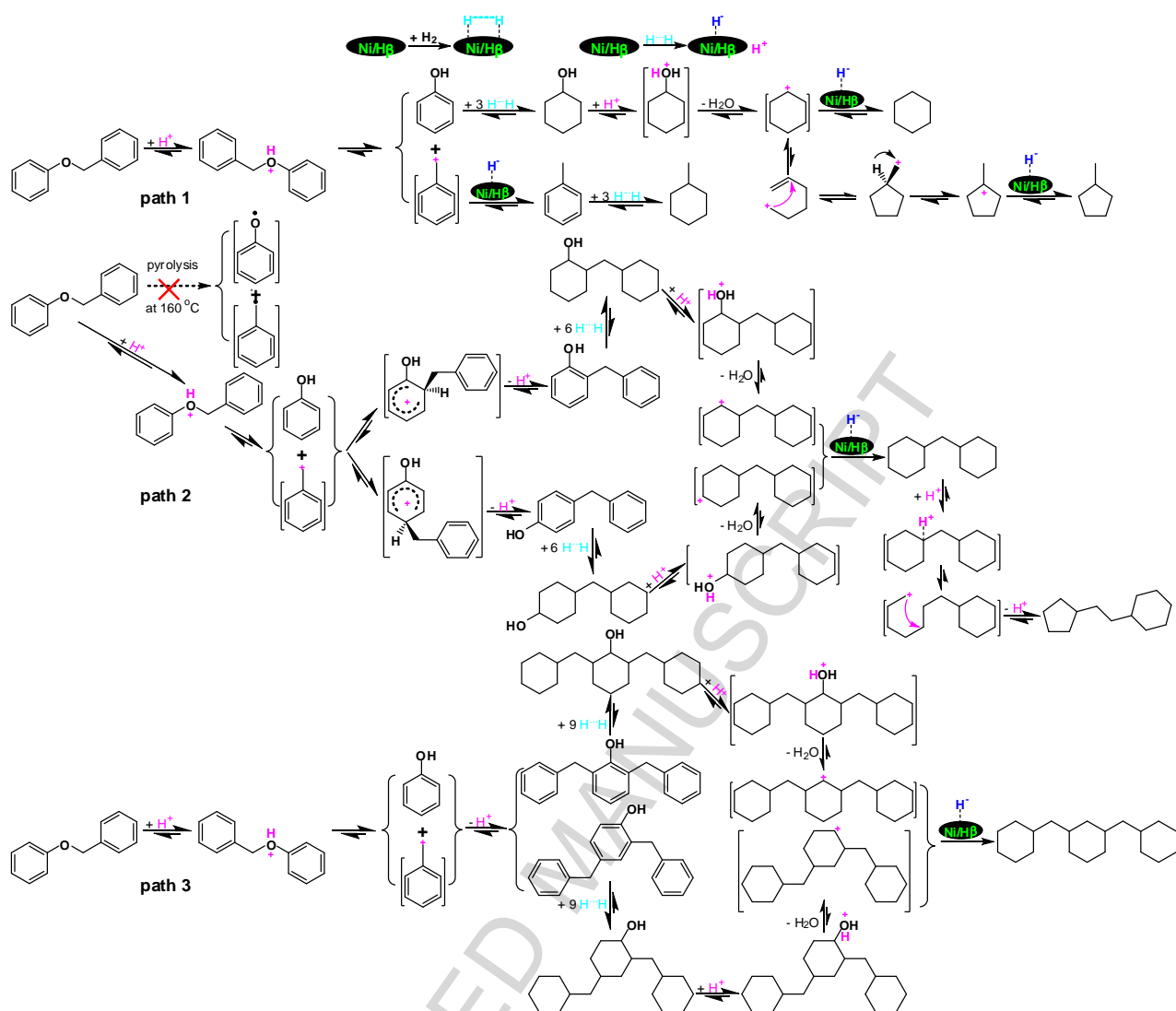


Fig. 3. NH₃-TPD profiles for different acidic zeolites and Ni₁₀%/Hβ.



Scheme 1. Possible pathways for **CHC** of **BOB** under H_2 atmosphere over $\text{Ni}_{10\%}/\text{H}\beta$.

ACCEPTED MANUSCRIPT

Table 1 CHC of BOB over supported Ni catalysts.

Catalyst	Conversion (%)	Product selectivity (%)												
		C H	M CP	M CH	Tolu ene	C H L	Phe nol	DC HM	CP EC	B C H	2-B CH	2-B PH	4-B PH	Tri mer s
Ni ₁₀ %/A C	95.5	1. 6		28. 3	29.0	33 .5	2.8							
Ni ₁₀ %/H ZSM-5	54.7	14 .9		26. 6	34.0	7. 9	16. 3							
Ni ₁₀ %/H β	100	7. 8	0.2	3.5	0.6		0.2	52.6	15. 7	8.5	3.0	3.2		4.7
Ni ₁₀ %/H Y	84.9	8. 2	0.3	4.3	18.5	0. 3	15. 0	12.0	0.4	3.6	1.5	27. 8	4.1	3.4

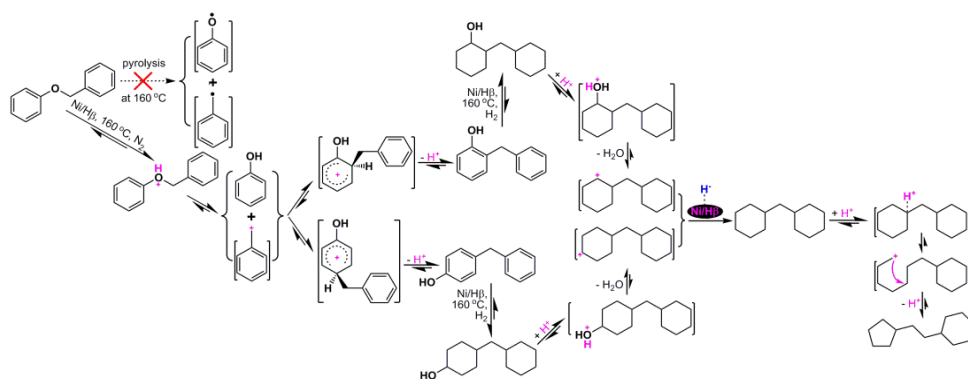
MCP: methylcyclopentane; CHL: cyclohexanol; BCH: benzylcyclohexane; 2-BCH: 2-benzylcyclohexanol; Trimers: including dibenzylphenols and 1,3-BCMC.

Table 2 CHC of BOB over Ni₁₀%/H β for different periods of reaction time.

Reaction time (min)	Conversion (%)	Product selectivity (%)								
		CH	MCP	MCH	Toluene	Phenol	DCHM	CPEC	BCH	2-BCH
10	80.0	5.9		1.7	3.8	3.0	15.4	1.7	3.9	1.5
30	100	6.7		2.0	2.6	1.9	24.5	3.2	6.7	2.7
60	100	7.7		2.4	2.4	1.5	31.4	4.7	8.7	3.5
90	100	7.7		2.8	1.7	0.7	41.5	9.9	8.8	3.0
120	100	7.8	0.2	3.5	0.6	0.2	52.6	15.7	8.5	3.0

H₂ atmosphere; MCP: methylcyclopentane; BCH: benzylcyclohexane; 2-BCH: 2-benzylcyclohexanol; Trimers: including dibenzylphenols and 1,3-BCMC.

Graphical abstract



Highlights

- Ni/H β was first found to be effective for converting BOB into bicyclic cycloalkanes (BCCs).
- BOB is quickly rearranged to benzylphenols and then further hydrodeoxygenated to BCCs.
- The selectivity of BCCs can be further improved with the pretreatment under N₂ atmosphere.